RSC Advances

PAPER

View Article Online
View Journal | View Issue

Cite this: *RSC Adv.*, 2017, **7**, 42800

Polyimide thin film composite (TFC) membranes *via* interfacial polymerization on hydrolyzed polyacrylonitrile support for solvent resistant nanofiltration

Shanshan Yang, [ab] Hongyan Zhen [ab] and Baowei Su *[ab]

Highly permeable, selective and solvent resistant nanofiltration (SRNF) membranes are desirable for the separation of substances on a molecular level in organic solvent. Polyimides have attracted significant attention for their chemical, structural and thermal stability. In this work, hydrolyzed polyacrylonitrile–polyamide acid (H-PAN/PAA) composite membranes were prepared *via* interfacial polymerization of *m*-phenylenediamine (MPD) and 1,2,4,5-benzenetetra acyl chloride (BTAC) on hydrolyzed polyacrylonitrile (H-PAN) supports. The formed H-PAN/PAA membranes were then transformed into H-PAN/PI thin film composite (TFC) membranes by a chemical imidization method. The effects of acetone as co-solvent in organic phase solution, the additives in the aqueous solution and the imidization time on the performance of the prepared PI TFC membranes were investigated. The chemical composition and the morphology of the prepared composite membranes were characterized by using FTIR, SEM and AFM. The hydrophilicity of the membrane surface was also measured. Using Rhodamine B (RB) with molecular weight (MW) of 479 dalton (Da) and Coomassie brilliant blue (CBB) G250 (MW = 854 Da) as model chemicals, the rejections of the prepared SRNF membranes for 100 mg L^{-1} of RB–ethanol solution and CBB G250–ethanol solution were about 92.8% and 99%, respectively. Their ethanol permeances were about 0.79 L m^{-2} h^{-1} bar^{-1} and 0.69 L m^{-2} h^{-1} bar^{-1}, respectively. After being immersed respectively into CCl_4, toluene, ethanol, acetone and methanol pure solvents for 30 days, the rejections of the prepared SRNF membranes remained quite stable.

Received 23rd July 2017
Accepted 30th August 2017

DOI: 10.1039/c7ra08133b

rsc.li/rsc-advances

Introduction

Organic solvent nanofiltration (OSN), also known as solvent resistant nanofiltration (SRNF), is a new burgeoning technology which holds enormous potential for the fine chemical, pharmaceutical, food and petrochemical industries as it allows separation of organic mixtures on a molecular level.[1] Compared with general separation techniques such as distillation, crystallization and adsorption, *etc.*, OSN process needs no phase transition, thus it can minimize the degradation of heat sensitive materials and avoid some unwanted side reactions, and in particular, reduce the energy consumption. Recently, more and more researchers have begun focusing their studies on the membrane materials and preparation methods for SRNF membranes.[2–20] Polymers involving polyacrylonitrile (PAN),[5,6,21] polyetherimide (PEI),[7–10] polysulfone (PSF),[11,12,22] polyphenylsulfone (PPSU)[14,15] and polybenzimidazole (PBI)[10,16,17] have been reported to prepared SRNF membranes. Various new methods and materials have been reported to prepare SRNF membranes.[18–20,23] For example, mixed matrix membranes were prepared using nanoparticles such as TiO_2 (ref. 23) and graphene oxide nanosheets[18] in the selective layer and they showed improved permeance and rejection.

Polyimide (PI) is one of the most widely used polymers in high temperature plastics, dielectrics, photoresists, nonlinear optical materials and separation membrane materials due to its chemical and thermal stability.[24] The use of PI in SRNF membrane preparation is increasing.

Most PI SRNF membranes were integrally skinned asymmetric (ISA) membranes fabricated by phase inversion, which possesses a skin-layer on the top of a porous sublayer with the same composition. A number of recent studies have been carried out on PI asymmetric SRNF membranes prepared through solidification of emulsified PI solutions *via* phase inversion.[2–4,17,25] Since PI can be dissolved in some strong polar solvents such as *N*,*N*-dimethylformamide (DMF), *N*,*N*-dimethylacetamide (DMAc), *N*-methyl pyrrolidone (NMP) and dimethyl sulfoxide (DMSO), which are typically used in membrane fabrication, the phase inversion membrane usually needed

[a]*Key Laboratory of Marine Chemistry Theory and Technology (Ocean University of China), Ministry of Education, 238 Songling Road, Qingdao 266100, China. E-mail: subaowei@ouc.edu.cn; Fax: +86 532 66786371; Tel: +86 532 66786371*

[b]*College of Chemistry & Chemical Engineering, Ocean University of China, 238 Songling Road, Qingdao 266100, China*

a post-treatment, such as imidization or cross-linking, to improve its solvent resistance. Wang *et al.*[2] reported the fabrication of PI SRNF membranes by a two-step method including the preparation of PAA membranes *via* phase inversion and the subsequent thermal imidization of PAA membranes. Vanherck *et al.*[26] reported PI membranes phase-inverted from PI solutions and subsequently cross-linked with *p*-xylylenediamine, which exhibited superior chemical stability in aprotic solvents. Nanoparticles were also used in the phase inversion membrane. Vandezande *et al.*[27] reported a kind of zeolite-filled SRNF membranes prepared with emulsified PI solution *via* phase inversion.

Just recently, thin film composite (TFC) membrane has been investigated by several researchers *via* coating selective top layer on PI substrate. Xu *et al.*[28] prepared a kind of composite membrane with a mussel-inspired polydopamine coating layer based on PI support. Sun *et al.*[29] prepared a dual-layer OSN hollow fiber membrane with hyperbranched polyethylenimine cross-linked polyimide as the inner support layer.

Interfacial polymerization (IP) is the most generally used method to prepare thin film composite (TFC) membranes consisting of an ultra-thin separating "barrier" on the top of a chemically different porous support.[1,30,31] However, most research work were focused on aqueous membranes. Jimenez Solomon *et al.*[32] reported that PI-based TFC membranes prepared with MPD and TMC by IP have the potential to achieve higher permeances than the polymeric asymmetric membranes, without sacrificing selectivity. To our knowledge, there is seldom any research work on PI selective layer made by IP process excepted that Yang *et al.*[33] had reported a kind of polyimide/polypropylene SRNF membrane fabricated *via* interfacial polymerization and chemical imidization. However, there is still little information available in literature about the fabrication of PI TFC membranes *via* IP process.

It is of great importance to prepare PI TFC membranes for SRNF with IP process which is environmental friendly, economic and simple. This is also of great significance for the further development and industrial applications of PI SRNF membranes. Hence, the aim of our study is to investigate the method of fabricating PI TFC membranes for SRNF *via* the IP process and further post-treatment.

In this work, we reported a new PI TFC membranes for SRNF prepared on hydrophilic polyacrylonitrile supports *via* the IP process and subsequent imidization process, as shown in Fig. 1. Several key preparation parameters of the PI TFC membranes were investigated, including additive agent in the aqueous solution, the addition of co-solvent in the organic solution, as well as the imidization time. The hydrophilicity of the membrane surface was measured. Various properties (surface morphology and structure) of the prepared PI SRNF membranes were extensively characterized by means of scanning electron microscopy (SEM) and atomic force microscopy (AFM). The separation performance of the prepared SRNF membrane was evaluated by the filtration of dye–ethanol solution. As the stability was very important for SRNF membranes in real OSN application,[3,17] the long term solvent resistance performance of the prepared SRNF membranes in different organic solvents

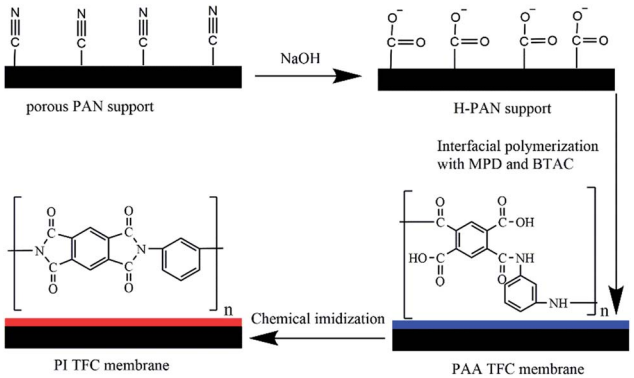

Fig. 1 Schematic of the fabrication procedure of the PI TFC membranes.

(CCl_4, toluene, ethanol, acetone and methanol) was also investigated.

Experimental

Materials

Polyacrylonitrile (PAN) ultrafiltration (UF) membrane with molecular weight cut-off (MWCO) of 50 000 dalton (Da) was purchased from Rising Sun Membrane Technology Co. Ltd., Shanghai, China. 1,2,4,5-Benzenetetra acyl chloride (BTAC, 97%) was purchased from Guangzhou Zhiya Chemdrug Technology Co. Ltd., Guangzhou, China. Tetrabutyl ammonium chloride (TBAC, 95%), Rhodamine B (RB, MW = 479 Da) and Coomassie brilliant blue (CBB) G250 (CBBG250, MW = 854 Da) were purchased from Shanghai Ourchem Reagent Co. Ltd., Shanghai, China. *m*-Phenylenediamine (MPD), sodium dodecyl sulfonate (SDS), acetic anhydride, acetone, trimethylamine (TEA), *n*-hexane, carbon tetrachloride (CCl_4), methanol, ethanol, toluene, sodium sulfate (Na_2SO_4), potassium carbonate (K_2CO_3), sodium hydroxide (NaOH) and potassium hydroxide (KOH) are all of analytical grade. They were purchased from Sinopharm Chemical Reagent Co. Ltd., China, and were used without further purification. Deionized (DI) water was used for membrane rinsing and preparation of aqueous solutions.

Pretreatment of the PAN UF membranes

Firstly, the commercial PAN UF membrane was immersed in DI water over night to eliminate any impurities and rinsed it by DI water for 1 minute before use. Then, the PAN membrane with 28.26 cm^2 effective area was immersed in NaOH solution (2.00 mol L^{-1}) at 65 °C for 1 h in order to convert the cyanide groups on the membrane surface into amide groups and further into carboxyl groups through hydrolysis (Fig. 2). Subsequently,

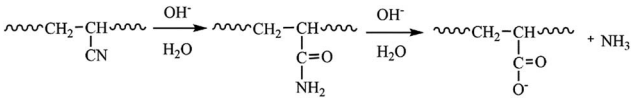

Fig. 2 Hydrolysis reaction of PAN support in alkaline environment.

the membrane was taken out and soaked, then was rinsed repeatedly and thoroughly with DI water to remove the excess NaOH solution until the pH of the soaking solution water became neutral. Finally, the hydrolyzed PAN (denoted as H-PAN) membrane was stored in DI water for further utilization.

Preparation of the PI TFC membranes

The H-PAN support membrane was immersed in the aqueous solution containing MPD (0.5 wt%), SDS (0.16 wt%), KOH (0–0.11 wt%), K_2CO_3 (0–0.2 wt%) and TBAC (0.1 wt%) for 20 min. After the excess aqueous solution was removed, the support was dried in the air until no droplets was seen on the substrate surface. Then the support was immersed into the BTAC organic solution (0.25% weight/volume BTAC and 0–0.8 wt% acetone in hexane) for 90 s to generate a nascent polyamide acid (PAA) composite membrane *via* interfacial polymerization. After that, the membrane was taken out again and dried in the air. The composite membrane was then immersed in the chemical imidization reagent (volume ratio of TEA : acetic anhydride : acetone = 1 : 3 : 10) at 40 °C for 0–24 h. Thus, the PI layer on the membrane surface was formed. Subsequently, the composite membrane was taken out and dried in the air. Finally, the membrane was rinsed by DI water and was soaked in DI water for storage.

According to the above steps, the optimal preparation conditions were obtained through several single factor experiments. For each test, at least 3 parallel membranes prepared under the same conditions were measured and all the data were the mean value of the measured data.

Characterization

The membrane morphology. The surface morphology of both the prepared PI TFC membranes and the H-PAN support membranes was investigated using a scanning electron microscope (SEM, S-4800, Hitachi Co., Japan). Prior to the characterization, the membranes were put into a vacuum drying oven at 40 °C for 24 hours, then the dried membranes were cut into appropriate size and were fixed on the object stage using conductive adhesive. After that, the SEM samples were sputter-coated using gold with a thickness of 5 nm on their surface. The surface morphology of the membranes was observed under 7 kV acceleration voltage in different magnification.

The two-dimensional (2D) and three-dimensional (3D) surface topographies of the prepared SRNF membranes were observed by Agilent 5400 type atomic force microscope (AFM, Nano-3D, Nikon Co., Japan) in tapping mode. The samples with the area of 5.0 μm × 5.0 μm were scanned using the dielectrophoresis tip under 1.0 Hz scanning frequency. The root mean square (RMS) roughness of the same membrane was determined based on three different regions using the computer software.

ATR-FTIR spectroscopy. The composition of the composite NF membrane surface was characterized by an attenuated total reflectance-Fourier transform infrared spectroscopy (ATR-FTIR, MAGNA-560, Nicolet, USA) under 2 cm^{-1} resolution at the spectrum range of 4000–600 cm^{-1}.

Surface hydrophilicity. The contact angle of the membrane surface was measured by the contact angle goniometer (DSA100, Kruss, Germany) with the static hanging drop method. 1.0 μL DI water was taken to deposit onto the surface of the sample in order to reduce the error of each sample. Each sample was measured at 6 different points with 5 mm interval per point. The contact angle was obtained by computer software and the arithmetic mean value was taken as the final contact angle.

Table 1 The polarity values of the organic solvents[34]

Solvent	CCl_4	Toluene	Acetone	Ethanol	Methanol
E_T (30)	32.4	33.9	42.2	51.9	55.4

Separation of inorganic salt solutions. The separation performance of the composite membranes for inorganic salt solutions was measured using a homed-made cross-flow system. Two stainless steel sinks with each effective area of 28.26 cm^2 were arranged in serial. The performance of each membrane sheet was tested at 1.0 MPa and room temperature, using 2000 mg L^{-1} Na_2SO_4 solution. The permeate flux was measured by using an electric balance and a computer data acquisition system, and it was stable after about 30 min running. However, to acquire accurate rejection value of the membranes, the permeate was sampled until after 1 h running. The electronic conductivities of the permeate and the feed were measured by a conductivity meter. Then, the rejections and the permeances were calculated according to literature.[31] For the reproducibility, we used at least three pieces of membrane sheets for each experiment. The average values were calculated for each test.

Separation of dyes in organic solvents. The separation performance of the prepared PI SRNF membranes for organic dyes with different molecular weights was investigated using 100 mg L^{-1} RB–ethanol solution and 100 mg L^{-1} CBBG250–ethanol solution, respectively, at 1.0 MPa and room temperature. The experimental procedure, the reproducibility, as well as the rejections and the permeances calculation were the same as those in the test of the inorganic salt solutions. The concentrations of the permeate and the feed solution were measured by a UV-visible spectrophotometer (UV-Vis, UV759, Shanghai Precision & Scientific Instruments Co., Ltd.) and were calculated based on Lambert–Beer Law.

Solvent resistance performance of the membrane. In order to investigate the solvent resistance of the prepared PI SRNF membranes, several organic solvents with different polarity values were selected, as shown in Table 1.[34]

The prepared PI TFC membranes were firstly immersed in different organic solvents for 30 days. After being taken out and rinsed thoroughly with ethanol, the membrane was immersed in ethanol for about 2–4 hours. Then, the separation performance of these composite membranes for different organic dye solutions was investigated respectively.

Result and discussion

Mechanism of the interfacial polymerization process

Fig. 3 shows the FTIR spectra of the H-PAN membrane, the H-PAN membrane after being covered with the aqueous MPD

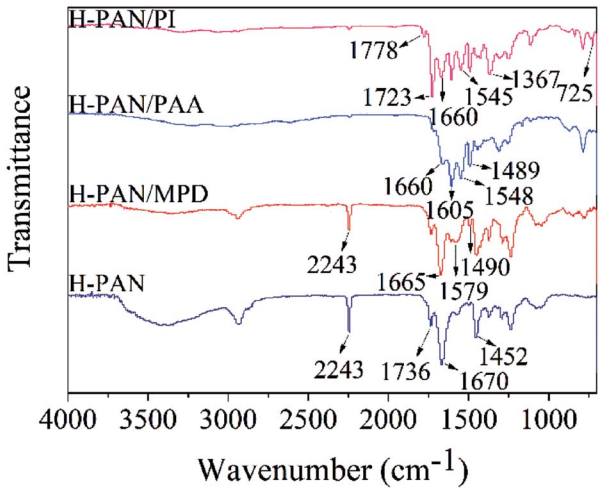

Fig. 3 FTIR spectrum of the H-PAN support and composite membranes.

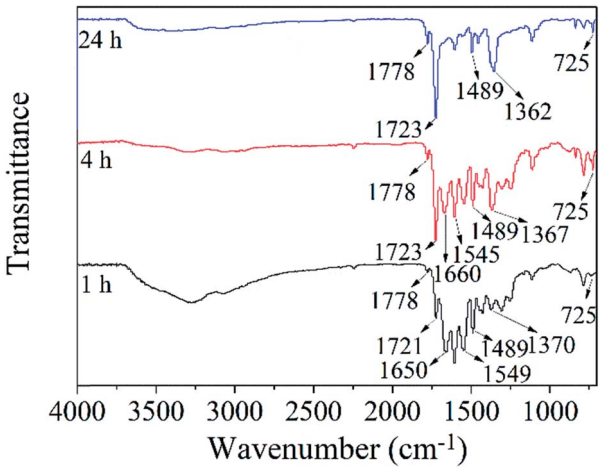

Fig. 4 FTIR spectra of the PI TFC membranes with different imidization time.

solution, the H-PAN/PAA membrane prepared *via* the IP process and the H-PAN/PI composite membrane prepared *via* chemical imidization under the optimal conditions.

For the H-PAN membrane, the characteristic absorption peak of C═O stretching vibration at 1736 cm^{-1} proved that the CN groups on the membrane surface had converted into carboxyl groups, which is similar to the previous reported studies.[35,36] The existing absorption peak at 2243 cm^{-1} corresponding to the CN groups indicated that the CN groups inside the H-PAN membrane didn't hydrolyze to COOH groups completely.[36] For the FTIR spectrum of the H-PAN support after being immersed in the MPD aqueous solution, the absorption peaks at 1665 cm^{-1} and 1579 cm^{-1} are the C═O stretches and the N–H stretches, respectively, and the absorption peak at 1490 cm^{-1} is the benzene skeleton stretches. They all indicated the deposition of MPD on the support surface. In the spectrum of the H-PAN/PAA membrane, the newly appeared absorption peaks at 1660 cm^{-1} and 1548 cm^{-1} correspond to the characteristic peak of the C═O stretches at amide I band and the characteristic peak of the N–H in-plane flexural vibration at amide II, respectively, which indicated that the CONH groups had generated through the amidization reaction between the NH_2 groups of MPD and the COCl groups of BTAC.[37] In the FTIR spectrum of the H-PAN/PI membrane, the absorption peaks at 1723 cm^{-1} and 1778 cm^{-1} correspond to the symmetric and asymmetric C═O stretches in the imide groups, respectively. The absorption peak at 1367 cm^{-1} is the C–N stretches. The absorption peak at 725 cm^{-1} corresponds to the imide carbonyl group stretches. All of them indicated obviously the cyclodehydration of amide groups and the formation of polyimide groups.[38,39]

Fig. 4 is the FTIR spectra of the prepared PI TFC membranes with different chemical imidization time (1 h, 4 h, 24 h). According to the spectra, the imide absorption peaks at 1723 cm^{-1}, 1778 cm^{-1} and 1367 cm^{-1} increase gradually with the imidization time increasing from 1 h to 24 h, while the amide absorption peaks at 1660 cm^{-1} and 1545 cm^{-1} decrease gradually. These phenomena indicated the increase of the imidization degree with imidization time. The amide absorption peaks at 1660 cm^{-1} and 1545 cm^{-1} vanished generally at 24 h imidization time, proving that the amide groups had converted into the imide groups completely.

Assuming that the imidization degree of the composite membrane with 24 h chemical imidization was 100%, the degree of chemical imidization at different imidization time was analyzed using the ratio of the absorbance at 1778 cm^{-1} and 1489 cm^{-1} according to literature.[37,40] The results were shown in Table 2. The imidization degree of the skin layer at 1 h imidization time was 22.6%. And it gradually increased up to 44.3% while the chemical imidization time increased to 4 h.

Factors influencing the PI TFC membranes performance

Effect of the co-solvent concentration. The separation performance of the PI TFC membrane prepared with different acetone concentrations (0.10, 0.25, 0.40, 0.60 and 0.80 wt%) in the organic monomer solution was investigated using 2000 mg L^{-1} Na_2SO_4 solution and 100 mg L^{-1} CBBG250–ethanol solution respectively. The results were shown in Fig. 5.

As presented in Fig. 5, with the increase of the acetone concentration, the permeances of the PI TFC membranes for both Na_2SO_4 solution and CBBG250–ethanol solution showed an upward trend. However, both Na_2SO_4 and CBBG250 rejections increased at first, they reached a maximum value when the concentration of acetone was about 0.25 wt%. Nevertheless, the rejections decreased generally with the further increase of the acetone concentration.

The reason for this phenomenon could be attributed to a narrow miscible zone formed in the hexane/water/acetone

Table 2 The imidization degree of the PI TFC membranes with the imidization time

Imidization time (h)	1	4	24
A_{1778}/A_{1489}	0.159	0.312	0.705
Imidization degree (%)	22.6	44.3	100

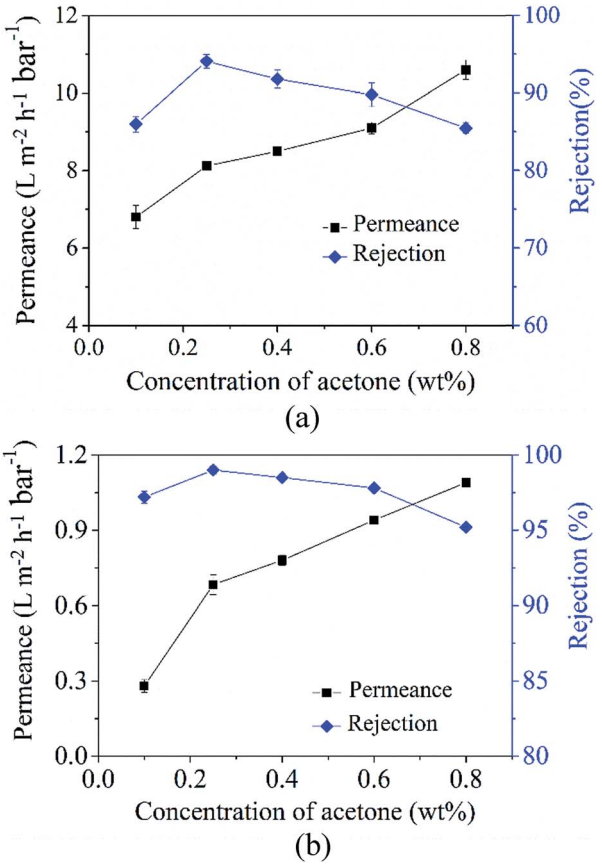

Fig. 5 Effect of concentration of acetone on the separation performance of the PI TFC membranes for Na_2SO_4 aqueous solution (a) and CBBG250–ethanol solution (b).

system during the IP process. This narrow miscible zone caused the formation of an orderly and regular active layer between the aqueous solution and the organic solution, resulting in the formation of a thinner skin layer and reducing the solvent penetration resistance.[41] Thus, the permeances of the composite membranes for both the aqueous solution and the ethanol solution increased greatly as acetone concentration increased. However, when the acetone concentration increased higher than 0.25 wt%, the skin layer formed in the IP reaction zone would become loose gradually due to the extension of the narrow miscible zone, causing the formation of larger pores on the membrane surface and the decrease of the densification of the skin layer.[41–43] Thus it resulted in the decrease of both Na_2SO_4 and CBBG250 rejections.

As depicted in Fig. 5, when the acetone concentration was 0.25 wt%, maximal rejection could be achieved for both the Na_2SO_4 aqueous solution and the CBBG250–ethanol solution, and the membrane permeance can be remained relative higher. Therefore, 0.25 wt% was selected as an optimal acetone concentration. Under this preparation condition, the rejection of the composite membranes for Na_2SO_4 solution could reach 94% with a permeance of 8 L m^{-2} h^{-1} bar^{-1}, and the rejection for CBBG250–ethanol solution could reach 99% with a permeance of 0.68 L m^{-2} h^{-1} bar^{-1}.

Table 3 Effect of acid acceptor on the separation performance of the PI TFC membranes

	Concentration	Na_2SO_4 solution	
Acid acceptor	(%)	Permeance (L m^{-2} h^{-1} bar^{-1})	Rejection (%)
K_2CO_3	0.2	6.9	88
KOH	0.1	6.11	89.6
K_2CO_3 + KOH	0.12 + 0.04	7.2	92.3

Effect of acid acceptor. As shown in Table 3, when the mixture of the strong alkali KOH and the weak alkali K_2CO_3 was added, both of the membrane permeance and the rejection increased. This may be explained by the fact that when only KOH was added, excess KOH would turn the aqueous monomer solution much strong alkali, KOH might react with BTAC molecules at the interface. Therefore, less BTAC molecules would participate in the IP reaction, and the extent of the IP reaction would be discounted, leading to a slight decrease of the membrane separation performance. On the other hand, when only the weak alkali K_2CO_3 was added, it might not have enough alkalinity to neutralize the acid generated during the IP reaction of MPD and BTAC. However, when both of them were added, K_2CO_3 can serve as a buffer solution so that the alkalinity of the solution would not be too high for KOH to react with BTAC. Therefore, we selected the mixture of K_2CO_3 and KOH as acid acceptors.

Effect of the imidization time. As shown in Fig. 6, when the imidization time was shorter than 4 h, the rejection increased with the imidization time, and the permeance had a reverse trend. However, when the imidization time was higher than 4 h, the rejection decreased sharply together with a sharply increase of the permeance accordingly. Therefore, the optimal imidization time was 4 h.

The effect of the imidization time on the membrane separation performance could be explained by the variation of the membrane sectional and surface morphology in the "SEM" section.

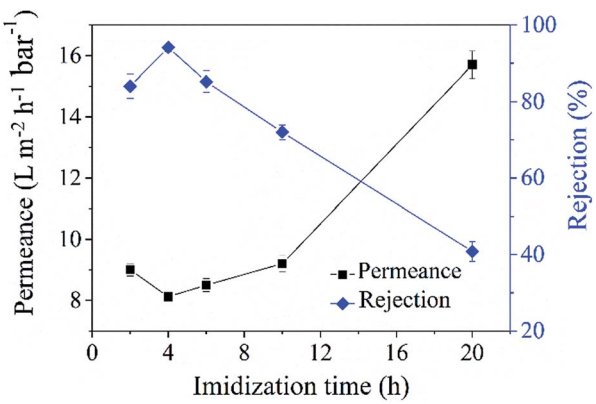

Fig. 6 The effect of imidization time on the separation performance of the PI TFC membranes for Na_2SO_4 aqueous solution.

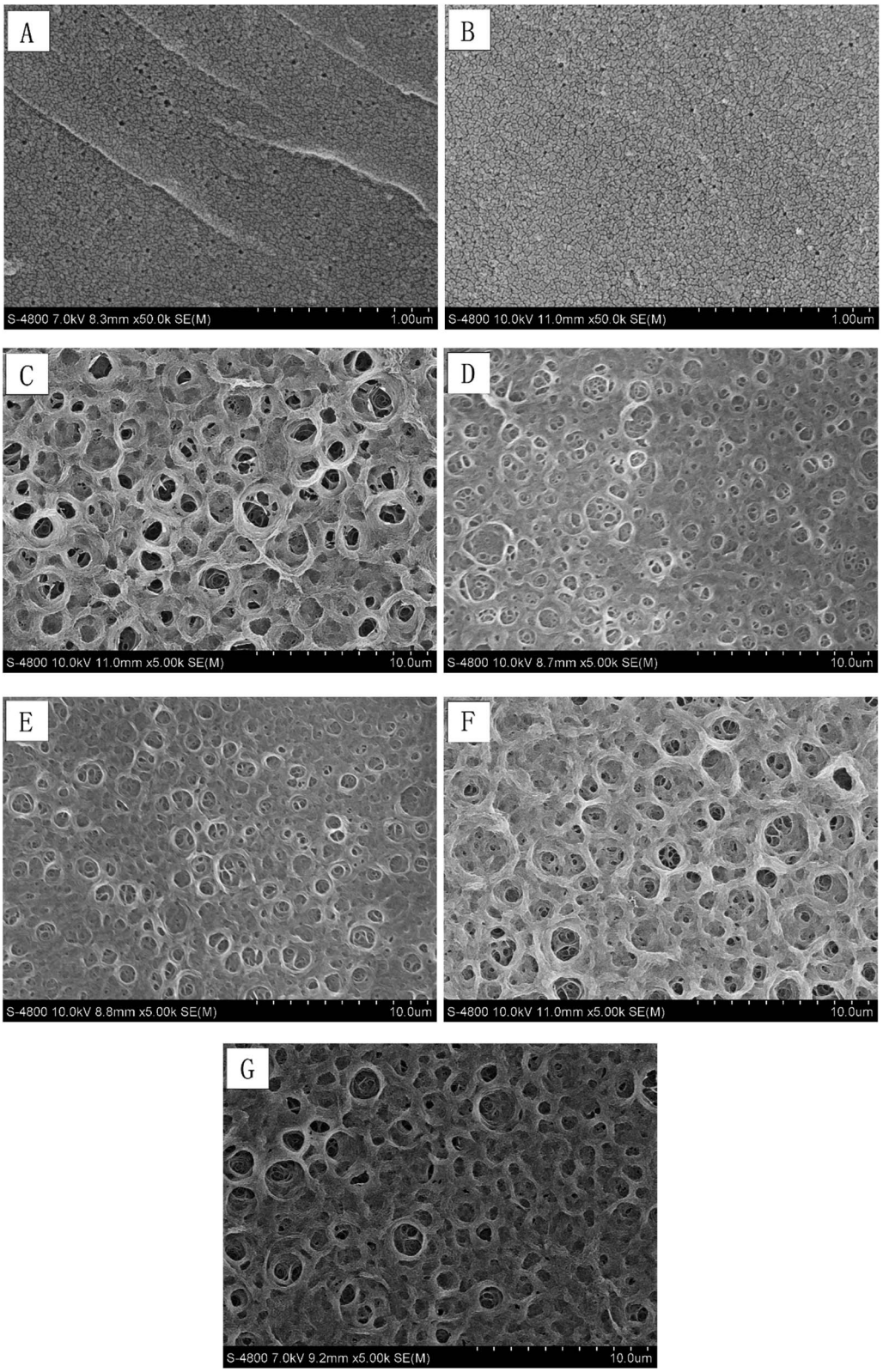

Fig. 7 SEM images of the membranes surface morphology ((A) PAN support; (B) H-PAN support; (C) PAA membrane; (D) PI membrane (imidization for 1 h, without acetone); (E) PI membrane (imidization for 4 h, without acetone); (F) PI membrane (imidization for 4 h, with acetone); (G) PI membrane (imidization for 24 h, without acetone)).

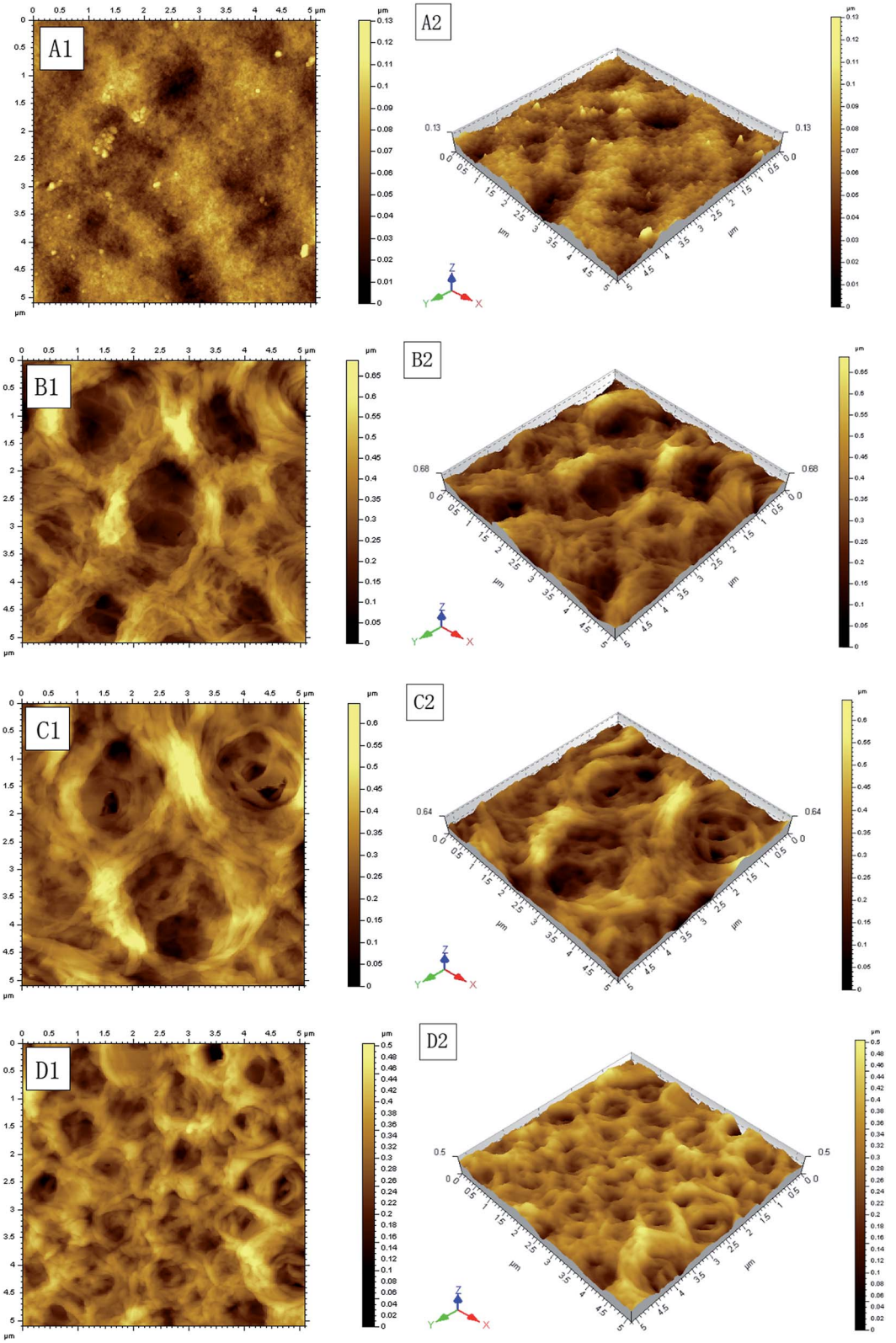

Fig. 8 AFM images of the membranes surface morphology (two dimensional: (A1) H-PAN support, (B1) PAA membrane, (C1) PI membrane (with acetone), (D1) PI membrane (without acetone); three dimensional: (A2) H-PAN support, (B2) PAA membrane, (C2) PI membrane (with acetone), (D2) PI membrane (without acetone)).

Characterization of the PI TFC membranes

SEM. As can be seen from Fig. 7, the membrane surfaces under different conditions showed different morphologies. From Fig. 7A and B, we can see that the surface of the PAN substrate membrane became smoother after being modified by NaOH solution. According to the SEM image in Fig. 7C, a kind of network structure was formed with apparent large pores on the membrane surface after the interfacial polymerization between MPD and BTAC. However, after 4 h chemical imidization, the membranes skin layer became dense, as can be seen in Fig. 7D.

Compared the images of Fig. 7D, E and G, when the imidization time was less than 4 h, with the increase of the imidization time, the pores size of the composite membranes became smaller and the density of them increased. The pores on the membrane surface for 4 h imidization were more uniform and denser, which indicated that the membrane surface morphology became better with the increase of the imidization time from 1 h to 4 h. However, with the further increase of the imidization time from 4 h to 24 h, there emerged much larger pore on the membrane surface, as can be seen from Fig. 7G. The morphology of the membrane surface can just provide evidence to the membrane rejection variation as illustrated in the "Effect of the imidization time" section, which showed a maximum value at the imidization time of 4 h.

The variation of the pore size with the imidization time can be explained by two main effects of the imidization reagent on the PI TFC membranes additional to the imidization reaction. The first is the swelling compression effects during the process of chemical imidization, which could remove the imperfections or defects in the membrane according to the Brown theory of latex formation.[44] This might play a leading role when the imidization time was less than 4 h, which caused the decrease of the pore size and increased the rejections, as shown in Fig. 6 and 7. The second can be termed as solvent activation effect, which was quite similar to the effects of the DMF solvent activation on the membrane performance reported in the literatures.[31,32,44] The chemical imidization reagent could remove some small molecular fragments formed during the interfacial polymerization step. It played a leading role when the imidization time was from 4 h to 24 h. Therefore, the pore size of the membrane became lager and the rejections decreased, as shown in Fig. 6 and 7.

The comparison of the membranes with and without the addition of acetone in the organic phase solutions during the IP process can be seen from Fig. 7E and F. The addition of acetone as co-solvent could adjust the morphology of the composite membranes,[42] leading to the appearance of larger ridge-valley structure and the increase of the pore size on the outermost layer.[43] However, the membrane could still maintain a high dye rejection with a slight increase of permeance, as shown in Fig. 5, revealing that the pores were not through-holes and there was a dense separation layer inside the skin porous layer. This has been proved by the commercial NF90 membrane which also has large pore-like structure on its surface[45] but still has a NaCl rejection as high as 90%, demonstrating a denser layer exists beneath the top rough layer.

AFM. As shown in Fig. 8A, the surface of the H-PAN support was smooth and the RMS value was about 15.4 nm. From Fig. 8B we can see that the surface of the PAA membrane without imidization was quite uneven, existing larger "vortex" structure with a RMS value of about 105 nm, indicating that the membrane surface was much rougher. From Fig. 8C we can see that the AFM image of the PI TFC membranes prepared with the addition of acetone as co-solvent under the optimum conditions was more uneven with a RMS value of about 124 nm. According to Fig. 8D, the RMS value of the PI TFC membranes without the addition of acetone in the organic solution was 61.4 nm. Hence, the addition of acetone increased the roughness and the specific surface area of the membrane, which could increase the permeance of the composite membrane.[46]

Contact angle analysis. The variation of the contact angle during different membrane preparation stages is shown in Fig. 9. It can be seen that the contact angle of the PAN membrane was 37°, but that of the H-PAN membrane was 29°, which indicated that NaOH modification could improve the hydrophilicity of the PAN support greatly. After the IP process, the contact angle of the PAA composite membrane increased quite slightly to 37.8°, this is due to the fact that the amide groups generated by the nucleophilic substitution reaction of MPD and BTAC are relative more hydrophobic than the COOH groups of H-PAN. Subsequently, imide groups were generated by the cyclodehydration of the amide groups, leading to the further decrease of the PI TFC membranes surface hydrophilicity. However, the contact angle of the PI TFC membranes increased only slightly to 42.5°, which indicated that the composite membranes have very good hydrophilicity and may have great potential for the applications in polar solvent.

Separation performance for dyes in organic solvents

From Fig. 10, the rejections and the permeances of the prepared PI TFC membranes for RB–ethanol solution were 92.8% and 0.80 L m^{-2} h^{-1} bar^{-1} respectively, and those for CBBG250–ethanol solution were 99% and 0.69 L m^{-2} h^{-1} bar^{-1}, respectively.

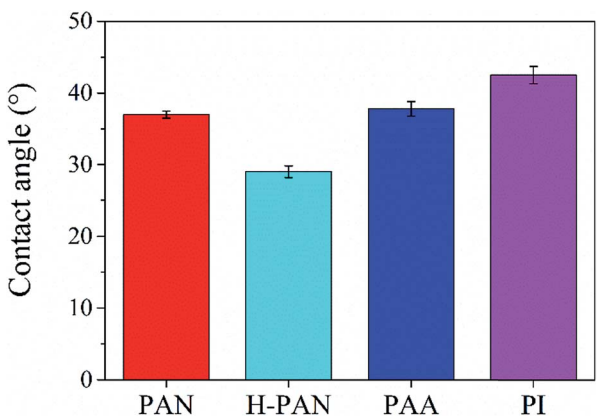

Fig. 9 The contact angle of the porous support and composite membrane surfaces.

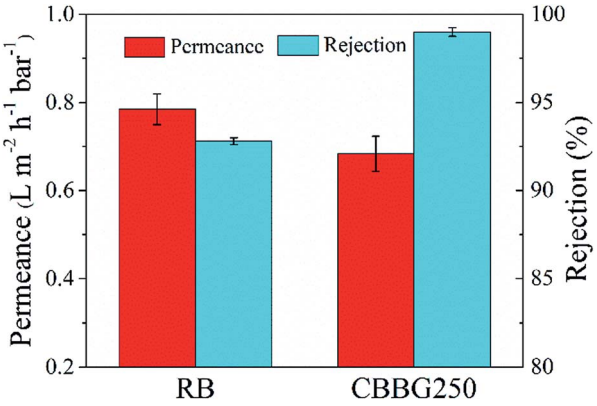

Fig. 10 The rejections and the permeances of prepared PI TFC membranes for different organic dye solutions.

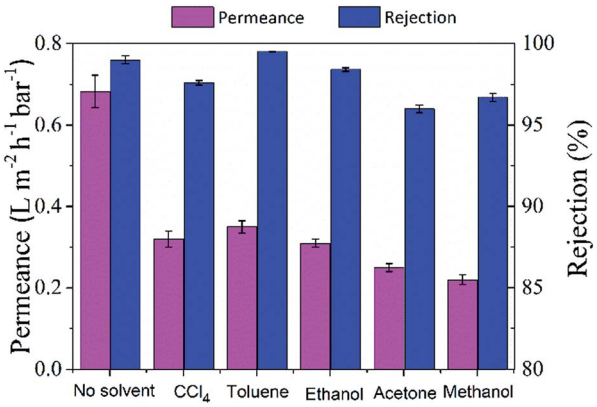

Fig. 11 The rejections and the permeances of the PI TFC membranes without soaking (no solvent) and after soaked in organic solvents (carbon tetrachloride, toluene, ethanol, acetone, methanol, respectively) for 30 days.

Table 4 compares the separation performance between the PI TFC membranes prepared in this work and others. The upper parts of Table 4 are those prepared without the addition of nanoparticles, and the lower parts are those with the addition of nanoparticles. It is obvious that the PI TFC membranes we prepared have good separation performance among the upper parts for dyes in the organic solutions, since we use even smaller solute with MW of 479 Da and 854 Da, yet we can achieve rejection of 99% for CBBG250 (854 Da) and 92.8% for RB (MW 479 Da), and the permeation flux is comparable. From the RB rejection we can estimate that the molecular weight cut-off (MWCO) of the PI TFC membranes prepared under the optimum conditions was about 450 Da.

Long term stability of the composite membranes in organic solvents

The long term stability of the PI SRNF membranes prepared under the optimal conditions were shown in Fig. 11.

According to Fig. 11, after being immersed in different pure organic solvents with different polarity index (Table 1) for 30 days, the ethanol permeances of the prepared TFC membranes decreased to about 50%. This was in accordance with some previous studies,[47,48] which indicated that the ethanol permeances of the pretreated membranes with different pure solvents showed a downward trend due to the chain reorganization.[47,48] This was a physical aging process in which the pore size and the pore density would be reduced, eventually causing the decrease of the permeances.[20] However, the rejections of the prepared PI SRNF membranes for CBBG250–ethanol solution only changed 0.5–3% after 30 days' immersion with these organic solvent, which proved that the PI SRNF membranes we prepared has very good solvent resistance performance and are quite promising in organic solvent system application.

Conclusions

We have successfully prepared PI TFC membranes for SRNF *via* interfacial polymerization between MPD and BTAC, with acetone as co-solvent introduced into the organic phase solution, and the subsequent chemical imidization. The prepared PI TFC membranes showed higher permeance without sacrificing rejections. The rejections of the prepared membrane for 100 mg L^{-1} RB–ethanol solution and 100 mg L^{-1} CBBG250–ethanol solution were about 92.8% and 99% with the permeances

Table 4 Comparison of the performance of the PI TFC membranes in this work with literature data

Membrane	Solvent	Permeance (L m^{-2} h^{-1} bar^{-1})	Solute and MW (Da)	R (%)	Reference
PI/H-PAN	Ethanol	0.79	Rhodamine B (479)	92.8	This work
PI/H-PAN	Ethanol	0.68	CBBG250 (854)	99	This work
EB-cross-linked PSU	Isopropanol	0.015	Rose bengal (1017)	94.3	49
Cross-linked (PDA/PI)	Ethanol	0.91	Rose bengal (1017)	99	28
(Catechol/POSS)/PAN	Ethanol	1.26	Rose bengal (1017)	99	19
(HAD/MPD/TMC)/PI	Ethanol	2.7	Rose bengal (1017)	100	50
p-Xylylenediamine/PI	DMF	5.41	Rose bengal (1017)	98	26
TPP/GO/HPEI/PSS	Ethanol	3.1	Rose bengal (1017)	97	18
MWCNTs-COOH/P84	Ethanol	9.6	Rose bengal (1017)	85	25
PPSU/Cu-BTC	Methanol	9.6	Methyl blue (800)	>90	15
GO-Poppy/PAN-H	Isopropanol	1.21	Rose bengal (1017)	99	51

of about 0.79 L m^{-2} h^{-1} bar^{-1} and 0.68 L m^{-2} h^{-1} bar^{-1} respectively.

After being immersed in organic solvents of CCl_4, methanol, ethanol and acetone for about 30 days respectively, the permeance of the PI TFC membranes for CBBG250–ethanol solution decreased by 50%. However, the rejections only changed 0.5–3.0%, which proved that the PI TFC membranes we prepared have very good solvent resistance performance and are quite promising in organic solvent system application.

Conflicts of interest

There are no conflicts to declare.

Acknowledgements

The authors thank the Natural Science Foundation of China (No. 21476218) for funding support. This is MCTL Contribution No. 151.

References

1 P. Vandezande, L. E. M. Gevers and I. F. J. Vankelecom, *Chem. Soc. Rev.*, 2008, **37**, 365–405.
2 J. Wang, K. Song, B. Cao, L. Li and K. Pan, *J. Chem. Technol. Biotechnol.*, 2016, **91**, 777–785.
3 H. Zhang, Z. Ren, Y. Zhang, Q. Yuan and X. J. Yang, *Chem. Eng. Commun.*, 2015, **203**, 870–879.
4 W. Dai, J. Yu, Y. Wang, Y. Song, F. E. Alam, K. Nishimura, C.-T. Lin and N. Jiang, *J. Mater. Chem. A*, 2015, **3**, 4884–4891.
5 S. Ilyas, N. Joseph, A. Szymczyk, A. Volodin, K. Nijmeijer, W. M. d. Vos and I. F. J. Vankelecom, *J. Membr. Sci.*, 2016, **514**, 322–331.
6 D. A. Musale and A. Kumar, *J. Appl. Polym. Sci.*, 1999, **77**, 1782–1793.
7 Y. Wang, L. Jiang, T. Matsuura, T. S. Chung and S. H. Goh, *J. Membr. Sci.*, 2008, **318**, 217–226.
8 I.-C. Kim, K.-H. Lee and T.-M. Tak, *J. Membr. Sci.*, 2001, **183**, 235–247.
9 X. Wu, L. Hao, J. Zhang, X. Zhang, J. Wang and J. Liu, *J. Membr. Sci.*, 2016, **515**, 175–188.
10 D. Chen, S. Yu, H. Zhang and X. Li, *Sep. Purif. Technol.*, 2015, **142**, 299–306.
11 A. K. Hołda, B. Aernouts, W. Saeys and I. F. J. Vankelecom, *J. Membr. Sci.*, 2013, **442**, 196–205.
12 V. Altun, J.-C. Remigy and I. F. J. Vankelecom, *J. Membr. Sci.*, 2017, **524**, 729–737.
13 A. K. Hołda and I. F. J. Vankelecom, *J. Membr. Sci.*, 2014, **450**, 499–511.
14 N. A. A. Sani, W. J. Lau and A. F. Ismail, *Korean J. Chem. Eng.*, 2015, **32**, 743–752.
15 N. A. A. Sani, W. J. Lau and A. F. Ismail, *RSC Adv.*, 2015, **5**, 13000–13010.
16 P. M. I. B. Valtcheva and A. G. Livingston, *J. Membr. Sci.*, 2015, **493**, 568–579.
17 I. B. Valtcheva, S. C. Kumbharkar, J. F. Kim, Y. Bhole and A. G. Livingston, *J. Membr. Sci.*, 2014, **457**, 62–72.
18 D. Hua and T.-S. Chung, *Carbon*, 2017, **122**, 604–613.
19 Y. C. Xu, Y. P. Tang, L. F. Liu, Z. H. Guo and L. Shao, *J. Membr. Sci.*, 2017, **526**, 32–42.
20 X. Q. Cheng, K. Konstas, C. M. Doherty, C. D. Wood, X. Mulet, Z. Xie, D. Ng, M. R. Hill, L. Shao and C. H. Lau, *ACS Appl. Mater. Interfaces*, 2017, **9**, 14401–14408.
21 A. V. Volkov, V. V. Parashchuk, D. F. Stamatialis, V. S. Khotimsky, V. V. Volkov and M. Wessling, *J. Membr. Sci.*, 2009, **333**, 88–93.
22 A. K. Hołda and I. F. J. Vankelecom, *J. Membr. Sci.*, 2014, **450**, 512–521.
23 X. Cheng, S. Ding, J. Guo, C. Zhang, Z. Guo and L. Shao, *J. Membr. Sci.*, 2017, **536**, 19–27.
24 D.-J. Liaw, K.-L. Wang, Y.-C. Huang, K.-R. Lee, J.-Y. Lai and C.-S. Ha, *Prog. Polym. Sci.*, 2012, **37**, 907–974.
25 M. H. Davood Abadi Farahani, D. Hua and T.-S. Chung, *Sep. Purif. Technol.*, 2017, **186**, 243–254.
26 K. Vanherck, P. Vandezande, S. O. Aldea and I. F. J. Vankelecom, *J. Membr. Sci.*, 2008, **320**, 468–476.
27 P. Vandezande, L. E. M. Gevers, N. Weyens and I. F. J. Vankelecom, *J. Comb. Chem.*, 2009, **11**, 243–251.
28 Y. Xu, F. You, H. Sun and L. Shao, *ACS Sustainable Chem. Eng.*, 2017, **5**, 5520–5528.
29 S.-P. Sun, S.-Y. Chan, W. Xing, Y. Wang and T.-S. Chung, *ACS Sustainable Chem. Eng.*, 2015, **3**, 3019–3023.
30 Y. Li, Y. Su, Y. Dong, X. Zhao, Z. Jiang, R. Zhang and J. Zhao, *Desalination*, 2014, **333**, 59–65.
31 M. F. Jimenez Solomon, Y. Bhole and A. G. Livingston, *J. Membr. Sci.*, 2013, **434**, 193–203.
32 M. F. Jimenez Solomon, Y. Bhole and A. G. Livingston, *J. Membr. Sci.*, 2012, **423–424**, 371–382.
33 Z. Yang, L. Zhang, G. Zhang and C. Li, *Journal of Chemical Industry and Engineering*, 2012, **63**(8), 2635–2641.
34 C. Reichardt, *Chemistry*, 1994, **94**, 2319–2358.
35 C.-L. Lai, W.-C. Chao, W.-S. Hung, Q. An, M. De Guzman, C.-C. Hu and K.-R. Lee, *J. Membr. Sci.*, 2015, **490**, 275–281.
36 G. Zhang, H. Yan, S. Ji and Z. Liu, *J. Membr. Sci.*, 2007, **292**, 1–8.
37 S. Hong, I.-C. Kim, T. Tak and Y.-N. Kwon, *Desalination*, 2013, **309**, 18–26.
38 J.-Y. Choi, W. Dong and Y.-H. Kim, *Colloids Surf., A*, 2008, **313–314**, 335–338.
39 K. Inomata, Y. Ozeki, S. Shimomura, Y. Sakamoto and E. Nakanishi, *J. Mol. Struct.*, 2005, **739**, 117–123.
40 M. B. Saeed and M.-S. Zhan, *Eur. Polym. J.*, 2006, **42**, 1844–1854.
41 C. Kong, M. Kanezashi, T. Yamomoto, T. Shintani and T. Tsuru, *J. Membr. Sci.*, 2010, **362**, 76–80.
42 C. Kong, T. Shintani, T. Kamada, V. Freger and T. Tsuru, *J. Membr. Sci.*, 2011, **384**, 10–16.
43 A. S. Al-Hobaib, M. S. Al-Suhybani, K. M. Al-Sheetan, H. Mousa and M. R. Shaik, *Membranes*, 2016, **6**(2), 1–13.
44 D. M. Ashish Kulkarni and W. N. Gill, *J. Membr. Sci.*, 1996, **114**, 39–50.
45 H. Guo, Y. Deng, Z. Yao, Z. Yang, J. Wang, C. Lin, T. Zhang, B. Zhu and C. Y. Tang, *Water Res.*, 2017, **121**, 197–203.

46 T. Kamada, T. Ohara, T. Shintani and T. Tsuru, *J. Membr. Sci.*, 2014, **467**, 303–312.
47 B. Van der Bruggen, J. Geens and C. Vandecasteele, *Chem. Eng. Sci.*, 2002, **57**, 2511–2518.
48 B. Van der Bruggen, J. Geens and C. Vandecasteele, *Sep. Sci. Technol.*, 2002, **37**, 783–797.
49 V. Altun, M. Bielmann and I. F. J. Vankelecom, *RSC Adv.*, 2016, **6**, 110916–110921.
50 S. Hermans, E. Dom, H. Mariën, G. Koeckelberghs and I. F. J. Vankelecom, *J. Membr. Sci.*, 2015, **476**, 356–363.
51 L. Shao, X. Cheng, Z. Wang, J. Ma and Z. Guo, *J. Membr. Sci.*, 2014, **452**, 82–89.